Peer reviewed version

Link to published version (if available):
10.1016/j.ndteint.2017.08.004

Link to publication record in Explore Bristol Research
PDF-document

University of Bristol - Explore Bristol Research
General rights

Ultrasonic Detection and Sizing of Compressed Cracks in Glass- and Carbon-Fibre Reinforced Plastic Composites

M. E. Ibrahim[1,2*], R. A. Smith[3], and C. H. Wang[4]

[1] Maritime Division, Defence Science and Technology Group, 506 Lorimer St, Fishermans Bend VIC 3207 AUSTRALIA.

[2] School of Aerospace, Mechanical and Manufacturing Engineering, RMIT University, Melbourne VIC 3001 AUSTRALIA

[3] Department of Mechanical Engineering, University of Bristol, Clifton, BS8 1TR, Bristol, UK

[4] School of Mechanical and Manufacturing Engineering, University of New South Wales, Sydney NSW 2052, Australia

*matthew.ibrahim@dst.defence.gov.au (corresponding author)

Abstract

Non-destructive evaluation of compressed cracks is a major challenge. A quantitative study of the effect of crack-tip closure on the pulse-echo ultrasonic sizing of delaminations in fibre-reinforced polymer-matrix composites (FRP) is presented. In particular, this study focuses on the interaction of ultrasound with a closed crack or kissing disbond, and their effect on the ultrasonic inspectability of FRP laminates consisting of carbon and glass plies. The compression of laminar cracks in these two different laminate types is clearly detectable via both pulse-echo and through-transmission ultrasonic measurements, but the reflected ultrasonic pulses in the two material types exhibit markedly different behaviour. The glass-fibre laminates show a drop in the reflected signal for crack openings up to approximately half the crack growth load, whereas the corresponding carbon-fibre laminates show the expected increase in the reflected signal as the crack opens. The origins of the observed effect of crack closure on the reflection and transmission of ultrasound are analysed in detail to ascertain possible mechanisms responsible for these effects.

Keywords

1   Introduction

Fibre-reinforced polymer (FRP) composites can be manufactured using a variety of raw materials that have anisotropic properties, configurations, and processes, making them a challenging subject for quantitative ultrasonic measurements. An understanding of the general applicability of various techniques for defect detection in FRP materials is well established, via ultrasonic inspection and many other methods [1-8]. In many cases, FRP materials are treated as simplistic homogeneous structures for the purposes of ultrasonic inspection, and thus inspected at low frequency and high power to overcome the high specific acoustic impedance in order to search for gross internal defects such as large voids and delaminations. However, defects arising in FRP are much more complex than their metallic counterparts, involving both matrix- and fibre-dominated cracking that depend strongly on the laminate structure, as well as residual stresses resultant from thermal and mechanical loading. One of the most prevalent and potentially critical types of damage is the separation ("delamination") of plies, leading to a significant reduction in local mechanical properties such as stiffness and load-carrying capacity, and can act as an initiation site for extensive further damage during operation. Delamination can arise in a range of scenarios, with foreign object impact being the main concern as its location depends on the service conditions, which makes it generally unpredictable at the design stage.

The highly anisotropic and inhomogeneous properties in the thickness direction cause a high degree of attenuation of acoustic waves, direction-dependent wave speeds, complex internal reflections, and mode conversions due to fibre-matrix interfaces and ply interface layers. In recent years, greater attention has been paid to the understanding of the interaction of ultrasound with the laminate components in order to perform thorough 3-D characterisation of FRP laminates [9].

The sensitivity of ultrasonic inspection to internal composite structure depends on the transmission and reflection of ultrasound at each interlaminar interface, which may be determined via the acoustic reflection coefficient for normal incidence, $R = (z_2 - z_1)/(z_2 + z_1)$, where z_N is the

specific acoustic impedance of each layer thick enough (comparable to the wavelength of the interrogating ultrasound) to interact with the transmitted ultrasonic compression wave, and is itself determined via measurements of the material parameters of density, ρ, and sound velocity, υ, via $z = \rho \times \upsilon$. While an ultrasonic inspection may be performed in a variety of physical configurations, the most straightforward and practical of these is the single-sided technique of contact pulse-echo inspection. In this case, a single piezoelectric transducer is placed above the inspection area at normal incidence and transmits a beam of compression waves into the specimen, then receives the reflected waves from the structure.

The presence of residual or built stress on in-service structures can force the closure of cracks [10,11], resulting in a reduction of the area over which a change in acoustic impedance reflects the ultrasound beam, and hence reducing the reflection response. This closure effect acts to mask the crack tip from the interrogating ultrasound wave, introducing a reduction in sizing accuracy, and can lead to the unfortunate error of underestimating the size and severity of the damage. This effect of this phenomenon on ultrasonic crack response signals has been demonstrated for metallic components used in high-end safety-critical applications such as aircraft or rail wheelsets [12,13]. In some cases, the problem can be mitigated by the application of appropriately directed loads in order to open cracks during an inspection, though this is generally impractical in many applications.

Fatigue-induced cracking in metallic beam or plate structures typically occurs in the orthogonal plane to the applied stress along the surface of the structure (Figure 1a), whereas in FRP laminates, macro-scale cracking is generally manifested as an interlaminar separation between successive plies in the lateral plane (Figure 1b). Added to this different crack geometry, the highly orthotropic properties of the plies complicates the propagation of ultrasound in the laminates.
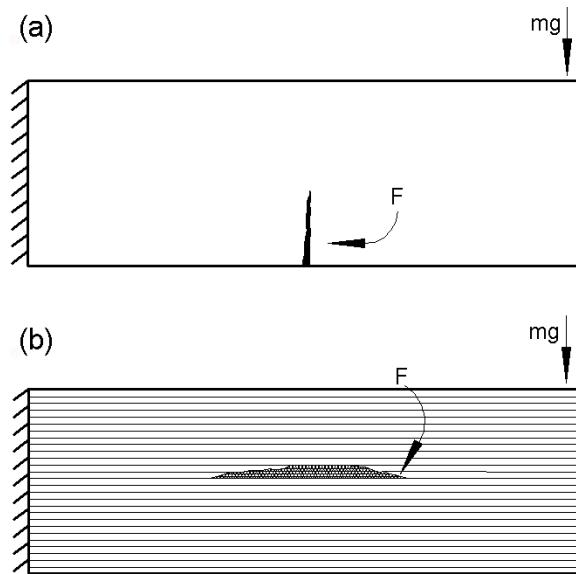
Figure 1. Schematic diagram depicting the crack closure problem in (a) a metallic beam, and (b) a composite laminate. Here, the loading due to gravity (mg) or other forces causes a compressive force F to act on the crack, resulting in closure.

In metallic alloys, the crack tip is generally well-defined when open, and provides a clear diffraction point for compression waves at ultrasonic frequencies. Interlaminar crack growth in FRP laminates is often characterised by fibre-bridging in the crack wake, between the two crack faces [14]. These bridging fibres give rise to a nonlinear spring-like behaviour that transmits different degrees of tensile and compressive loads in the through-thickness direction. In FRP structures such as curve beams and T-joints, the through-thickness (normal to ply interfaces) compressive stress may arise from built-in loads or static external loads, which cause delamination cracks to close. This closure would effectively turn part or possibly all of a delamination into a zero-volume kissing disbond: bond surfaces are in close contact but can transmit very little or zero tensile load.

There is also an inherent uncertainty in delamination or crack tip measurement irrespective of the material due to the physical dimensions of ultrasonic transducer elements. During practical inspection, the tip is defined as the point at which the ultrasonic echo from the back wall of the

specimen is half the amplitude due to scattering by the crack [15]. However, the 6 dB rule is often not able to size a delamination accurately, due to the presence of crossed-over fibres and uncracked ligaments of the matrix that may partially transmit ultrasonic waves. The potential effects of the unloading/reloading process in damaged composites on NDT methods was previously raised by Chen *et al.* [16], in which a full-field acoustography technique was applied to the real-time, in-situ monitoring of delamination growth in carbon/epoxy FRP laminates subjected to fatigue loading. While they were able to monitor the growth of delaminations under single-axis loading, this study did not provide insights into the effect of the applied loads on the inspection technique.

In this paper, we study the reflected and transmitted ultrasonic waves at the tip of a delamination in unidirectional carbon and glass FRP laminates, while applying a varying tensile load to open the delamination. Unidirectional laminates, while less representative of realistic structures than quasi-isotropic composites, were selected in order to reduce the complexity of laminate orthotropy with multiple fibre angles. The results demonstrate the effect of crack-closure on both the reflected and transmitted ultrasonic wave in glass- and carbon-fibre reinforced composites.

2 Experimental Method

2.1 Specimen fabrication

Carbon/epoxy and glass/epoxy laminates were fabricated using VTM264/HS-200 UD prepreg and MTM57/1062-300 E-glass UD prepreg respectively. The carbon/epoxy prepreg sheet was 200 gsm, with a fibre weight fraction of 0.62 and volume fraction of 0.53. The glass/epoxy prepreg ply was 300 gsm, having a fibre weight fraction of 0.65 and volume fraction of 0.49. Composite laminates consisting of 50 unidirectional plies were autoclave-cured at a temperature of 120°C and pressure of 90 psi. The resultant laminates were approximately 10 mm (carbon) and 13 mm (glass) thick. Hence their respective ply thicknesses were approximately 0.2 mm and 0.26 mm. Crack-starters were introduced at one end of the laminate by inserting a PTFE layer at the midplane of the laminate.

2.2   Initial crack growth

The composite laminates were cut into suitable test specimens using a diamond-tipped saw and prepared for crack growth under static loading. The specimens were oriented such that the fibre direction was aligned along the length of the specimen so that the crack would grow along the fibre direction. Five carbon/epoxy (C1 – C5) and six glass/epoxy specimens (G1 – G6) were manufactured and used in the experiments. The initial crack was further grown into the specimens via a double cantilever beam (DCB) test configuration to a length of approximately either 110 mm, or 115 mm, resulting in a crosshead-to-crack tip length of approximately 98 ± 1 mm or 103 ± 1 mm respectively. Testing was performed in accordance with the ASTM test standard for Mode I interlaminar fracture toughness [17]. Figure 2 shows a carbon-fibre specimen undergoing crack growth measurements in the test machine. Despite the varying material properties of the carbon/epoxy and glass/epoxy specimens, the load required to propagate the initial crack along the beam was similar, being 240 ± 10 N.

Figure 2. Carbon/epoxy laminate specimen undergoing static crack growth via DCB testing. The dimensions of the specimen are approximately 220 $\times$ 25 10 mm.

2.3   Ultrasonic characterisation of the initial crack

An ultrasonic inspection was performed on each specimen using a 5 MHz transducer (details given in Section 0) to characterise the tip region of the initial crack. Figure 3 shows a schematic diagram of the inspection setup and a detailed cross-section ('B-scan') of the ultrasonic echoes around the crack

tip, received from within a typical carbon/epoxy specimen. The specimen was not under any load during this initial inspection. The length of the crack shown in the image is approximately 25 mm, and the region of interest for the closed crack inspection is bounded by the dashed line at the tip of the visible part of the crack.
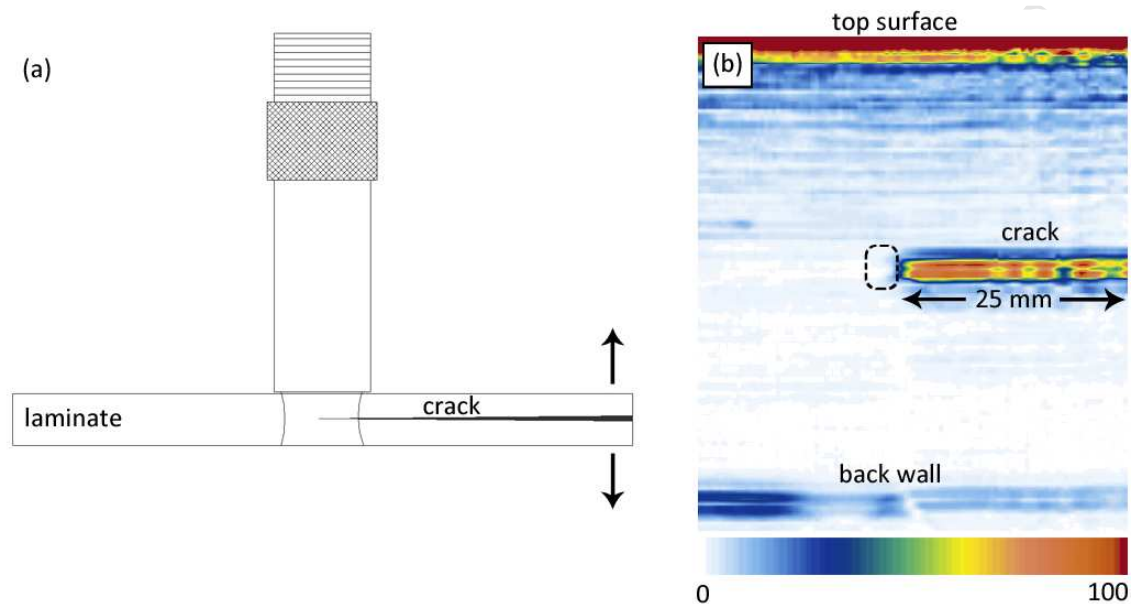

Figure 3. (a) Schematic diagram of the inspection performed at the crack tip, and (b) Typical cross-section ("B-scan") of the ultrasonic echoes detected from the specimen, relative strength shown on the graded colour palette. Notice the reduction in back wall echo strength over the crack region. The dashed box shows an approximate region of interest for this study, beyond the clearly identifiable reflection.

2.4   Ultrasonic inspection of the crack tip

Once the initial characterisation had been performed for each specimen, further measurements were made using *Olympus/Panametrics V201* 6 mm-diameter element, unfocused contact transducers. The transducers had a notional resonant frequency of 5 MHz. The crack tip was defined using the standard 6 dB drop method, at which a 50% reduction in signal amplitude occurred.

Once the crack tip location had been determined with the specimen in the unloaded state, the transducer was spring-clamped to the surface to ensure it remained in position. The specimen was

then returned to the test machine in the same static loading configuration as was used to grow the

initial cracks, and the crack progressively opened in order to measure changes to the ultrasonic

reflection from the crack tip. The opening load was gradually increased to a maximum of

approximately 80% of the load required to propagate the crack, ensuring no further crack

growthduring the ultrasonic measurements. The test machine crosshead was used to parameterise

the opening of the crack, which was done in 0.5 mm increments. The micromechanical effect at the

crack tip at each crosshead opening was not determined. Ultrasonic measurements were made both

in pulse-echo (single-sided) and through-transmission (send and receive transducers on opposite

sides of the specimen) modes. Material properties relevant to the ultrasonic inspection are given in

Table 1. The annotation follows the convention of Smith [18], in which the *3*-axis is defined as the

longitudinal fibre direction, and the *1* and *2* axes are orthogonal.

Table 1. Principal stiffness constants and characteristic specific acoustic impedance for typical carbon

and glass FRP components. Acoustic impedance values determined in-house.

Component	c_{11} (GPa)	c_{22} (GPa)	c_{33} (GPa)	z_0 (x10^6 N.s/m^3)
Carbon/epoxy [19]	13.22	13.22	155.17	5
E-Glass/epoxy [20]	17	17	45	11
Epoxy (neat) [21]	3.93	3.93	3.93	3

The carbon/epoxy laminate can be considered as transversely isotropic and has far higher stiffness

than glass/epoxy in the fibre direction (Table 1), but in the through-thickness direction the

glass/epoxy laminate has much higher stiffness owing to the far higher transverse modulus of glass

fibres (~50 GPa) compared to carbon fibres (~15 GPa). This higher transverse stiffness in the

direction of ultrasound propagation, combined with the thin epoxy resin layer at the interface region

between adjacent plies, results in a greater acoustic impedance mismatch in glass/epoxy laminates

9

than carbon/epoxy laminates. Hence, the power required to penetrate the same depth of glass-fibre composites is typically an order of magnitude greater than that for carbon-fibre composites, contributing to the difficulties in quantitative ultrasonic diagnosis of glass-fibre composites.

The combination of composite ply and the resin-rich interface layer between plies results in a half-wavelength-per-ply (half-wave) resonance [22], visible as minor echoes in the waveform. The greater stiffness gradient at the interface between the glass/epoxy ply and the resin interface layer also causes a marked increase in the prominence of the minor echoes in these laminates.

3 Results

3.1 Ultrasonic probe signal

The typical ultrasonic pulse incident on the laminate specimens (measured in water) is given in Figure 4a. The transducer is designed to produce a broadband response in order to limit the amount of ring-down at each interface, thus increasing the lateral resolution (ability to discriminate between closely spaced through-thickness layers). The signal shown was produced and measured by a broadband 5 MHz unfocused contact transducer, chosen to minimise 'ring-down' of the signal. Figure 4b shows the frequency spectrum of the signal, indicating a bandwidth of approximately 7 MHz, and a centre-frequency of 6.2 MHz.
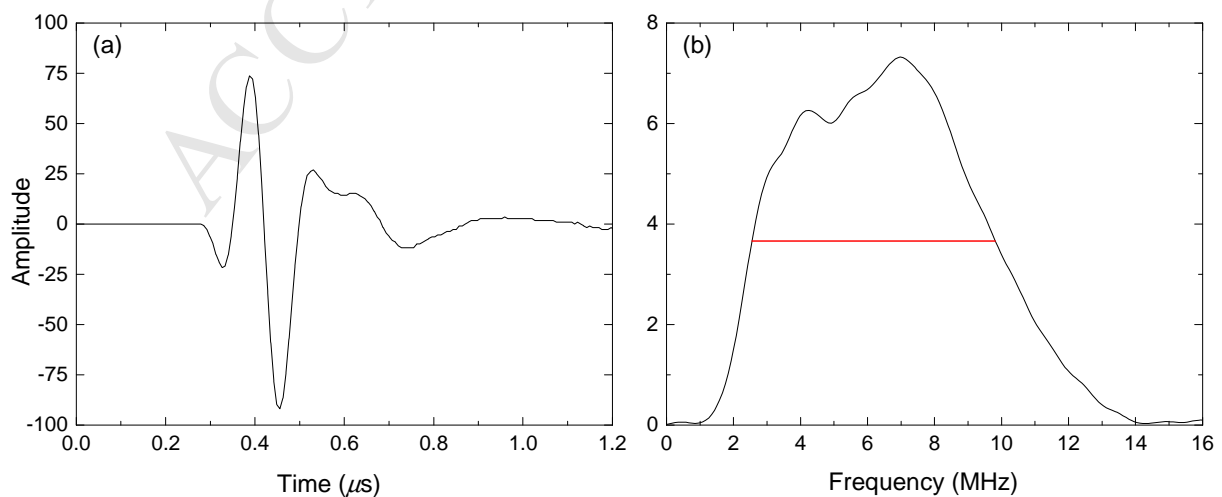

10

Figure 4. (a) Typical ultrasonic signal emitted by the piezoelectric transducers used in the study, as measured in water. (b) Frequency spectrum of the transducer signal, (red line – FWHM bandwidth).

3.2 Ultrasonic crack tip reflections

Typical ultrasonic reflections obtained at the crack tip for a single-element pulse-echo inspection are shown in Figure 5, for the typical carbon and glass laminates tested. The large echo at the composite-crack interface is due to the correspondingly large acoustic impedance mismatch between the composite material and air. A distinct difference in the response from the crack tip region, and the frequency content for the glass/epoxy and carbon/epoxy laminates is obvious, with much more significant internal response occurring throughout the thickness of the glass/epoxy specimen.
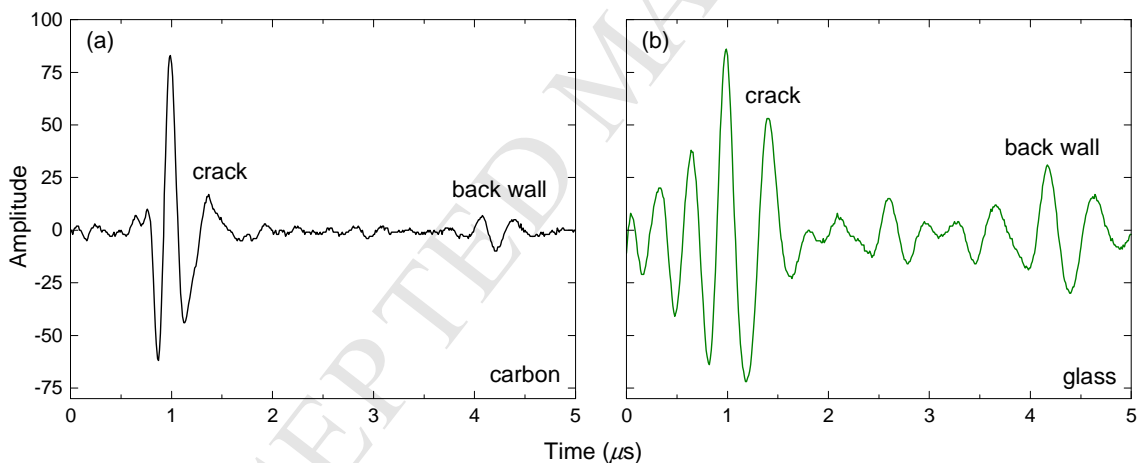

Figure 5. Typical signals obtained from pulse-echo inspection over the crack tip in the unidirectional (a) carbon/epoxy specimen C2 and (b) glass/epoxy specimen G4. Specimens were not under load.

3.3 Effect of composite crack closure on ultrasonic measurements

The anticipated outcome of the pulse-echo measurements is a gradual *increase* in the reflected crack tip signal as the crack is opened. Bridging fibres will gradually lose their load-carrying capacity so that the full impedance mismatch of the composite-air interface will be realised. In through-

transmission inspections, the expected result is a gradual *decrease* in transmitted sound energy, due to the increased reflection from the crack.

Results showing the effect of crack opening/closure on the ultrasonic transmission through carbon and glass composites using the experimental method presented in 0 are shown in Figure 6, for a number of incremental 0.5 mm crosshead openings. The signal has been truncated to show only the waveform corresponding to the reflection from the region close to the crack tip. The consecutive increments of crack opening were linear, and designed such that the test machine crosshead-to-crack tip displacement would be the same for each test specimen. The amplitude scale for the Figure was set arbitrarily, given the significant increase in ultrasonic energy required to penetrate glass/epoxy laminates compared to carbon/epoxy, and the relative difference in ensuing echo strengths.
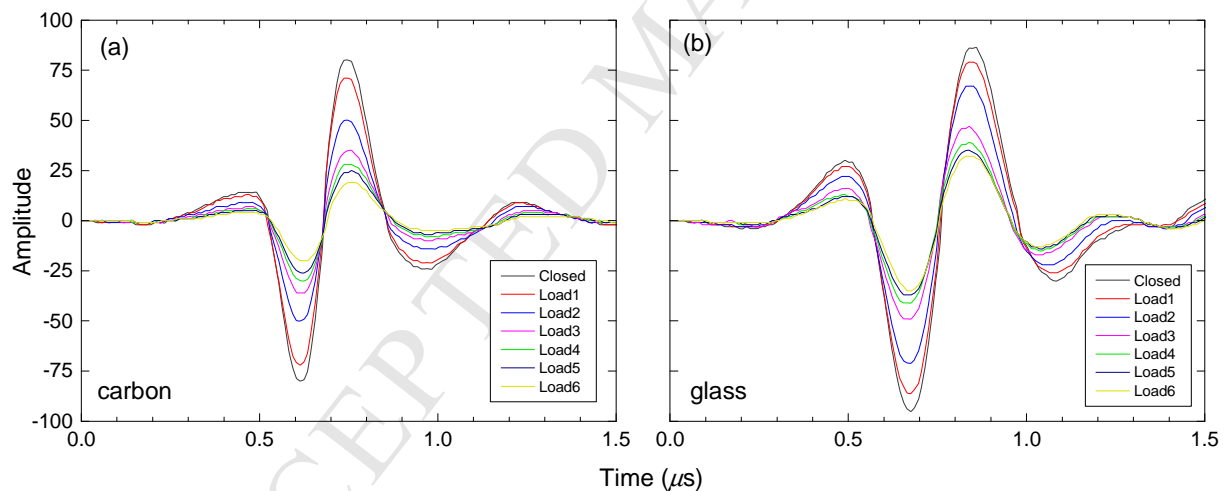

Figure 6. Typical ultrasonic transmission measured during opening of the laboratory-grown interlaminar crack in (a) carbon/epoxy specimen C2 and (b) glass/epoxy specimen G4. The amplitude scales for the two types of composite have been arbitrarily chosen for convenience of comparison.

Similar qualitative behaviour was measured for both material systems, in which the magnitude of the increments gradually decreased as the crack reached a maximum opening (limited by the load at which further crack growth would ensue). There is an immediate effect on the amplitude of the

transmitted signal due to the opening of the crack, whereby the amplitude of the signal is reduced

over several increments of crosshead displacement/opening. At higher loads, the probe tilt between

the two transducers may become significant enough to noticeably reduce the transmission

coefficient and thus the transmitted signal. The amplitude profiles for the two types of composite

are shown in Figure 7, where each laminate type is normalised to a value of 100% at zero load. The

scatter in the results obtained during the measurements was plotted as the uncertainty limits

surrounding the mean values for the carbon and glass laminates in Figure 7 (shaded zones). This

indicates a clear and repeatable crack closure effect on the ultrasonic signal transmission over a

crack tip for both the carbon/epoxy and glass/epoxy laminates, which decreases gradually with crack
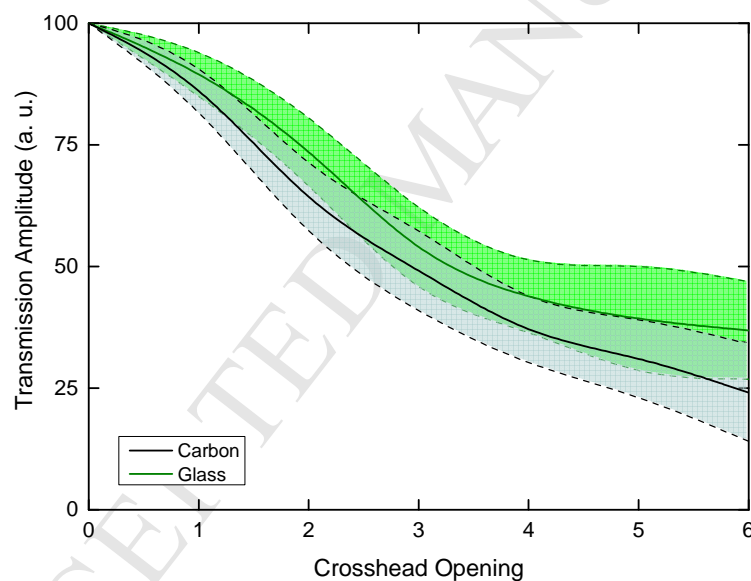
opening.

Figure 7. Reduction in ultrasonic transmission through the complete series of unidirectional

carbon/epoxy and glass/epoxy laminate specimens. Average values are plotted in each case, with the

extrema plotted in the shaded zones.

After performing pulse-echo measurements on the same set of specimens, a curious result was

immediately obvious (Figure 8). In the carbon/epoxy laminates, the magnitude of the reflected wave

increases immediately upon opening the crack. However, in the case of glass/epoxy laminates, the

magnitude of the reflected wave unexpectedly decreased initially, until the crack opening reached

approximately 60% of the peak value, and then increased as shown in Figure 9. This effect was

observed over a range of test frequencies on all the glass/epoxy laminate specimens. To our

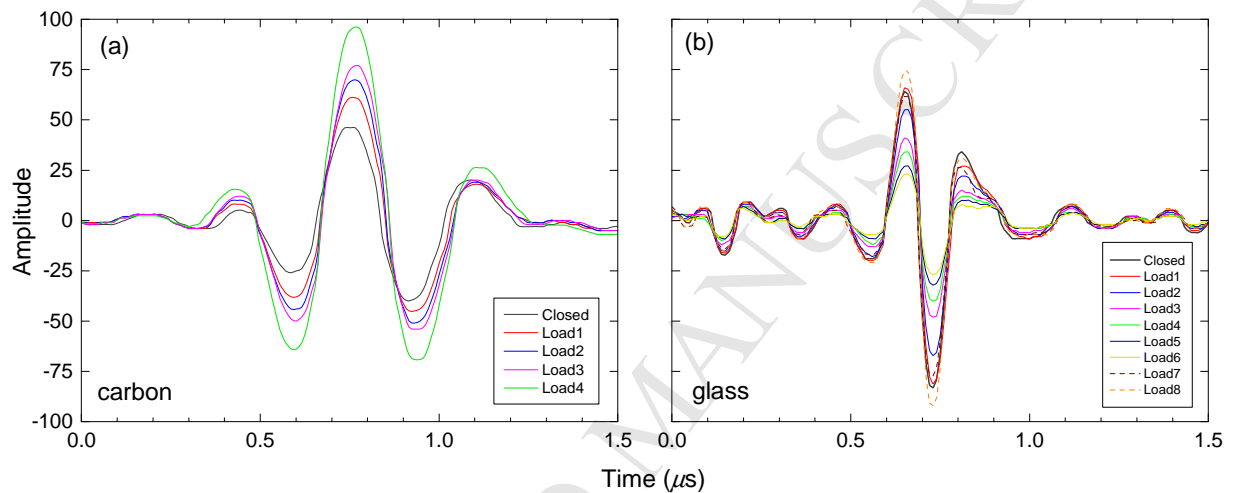knowledge, such behaviour has not previously been reported.

Figure 8. Typical ultrasonic pulse-echo reflection from the crack tip of the laboratory-grown

interlaminar crack in (a) carbon/epoxy specimen C2 and (b) glass/epoxy specimen G4. Higher

crosshead openings in the glass laminate are shown with dashed lines.
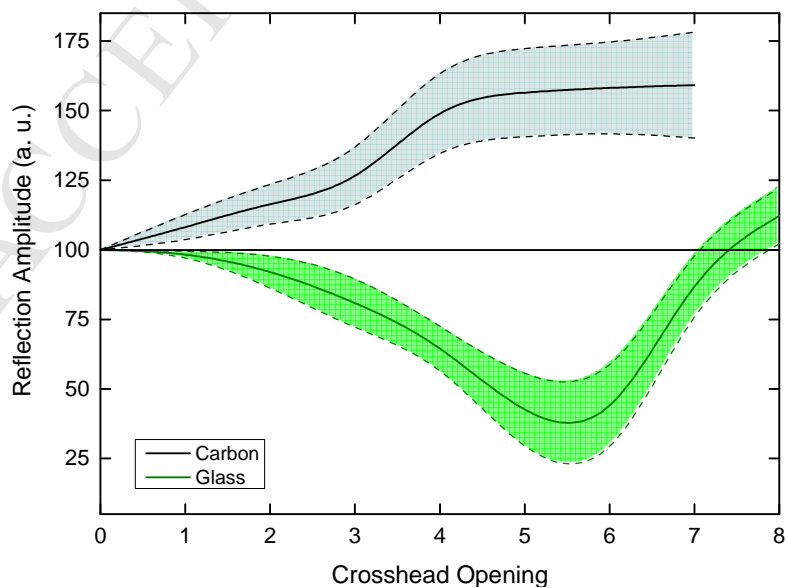
Figure 9. Relative ultrasonic pulse-echo response from the crack tip during crack closure/opening for the complete series of carbon/epoxy and glass/epoxy composites. The expected closure effect occurs for the carbon composite, whereas an opposite effect of a reduction in reflected ultrasound occurs initially in the glass composite, prior to being overtaken by the air-backed layer.

3.4   Microscopic surface examination

To better understand the microstructural behaviour of the fractured composite at the crack tip, and to provide a possible cause for the glass/epoxy laminate pulse-echo ultrasonic response, a detailed examination of the crack surfaces in the unidirectional carbon- and glass-fibre composites was performed using micro/nano-computed tomography (CT) and scanning electron microscopy (SEM). The crack tips were examined using a *GE Phoenix v|tome|x m-industrial* CT scanner, with the assistance of the *Volume Graphics VGStudio Max* analysis software. To facilitate sufficient x-ray penetration and to improve the visualisation of the crack tips, small (~3 mm) sections of the fracture surface were cut out of the bulk specimens.

Figure 10 shows an image of a crack in a carbon/epoxy composite laminate, without any load applied, and a series of crack front images at various slices approaching the crack tip. The length of the crack shown spans approximately 3 mm, the part of the crack that was covered by the transducer face in the measurements made in this study.
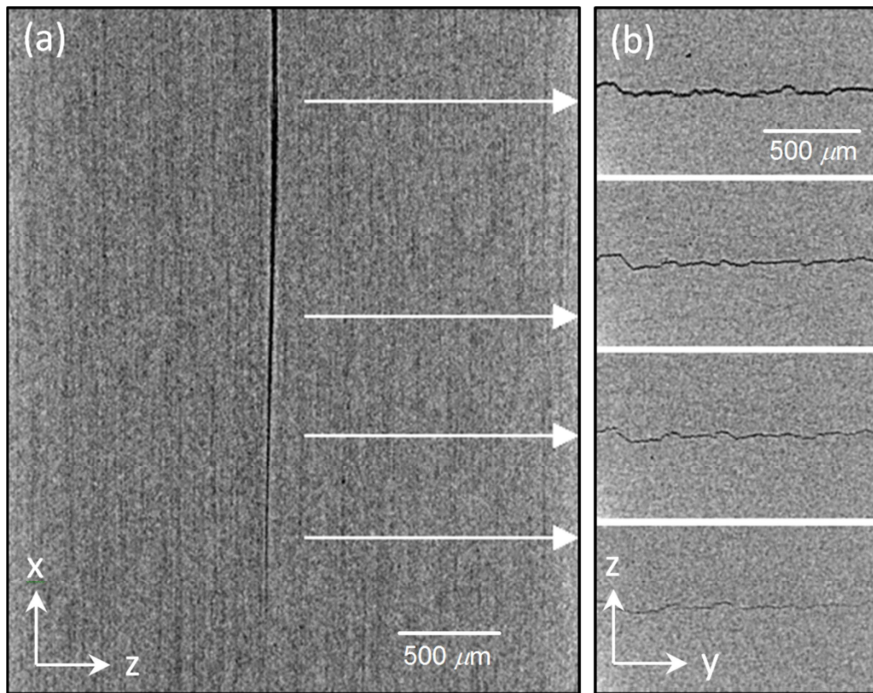
15

Figure 10. Nano-CT images of the crack in a carbon/epoxy laminate, viewed (a) along the length of the crack approaching the tip, and (b) Corresponding orthogonal images of the crack tip for the four slices shown along the crack. The crack length in (a) is approximately 3 mm, and the crack fronts in (b) are approximately 1.5 mm in length.

The SEM examination was performed using a *JEOL JSM-6490* instrument with an open crack surface that was prepared by forcibly opening the specimen after the load testing was complete. Images of the crack surfaces of the different composite laminates at an identical series of magnifications are given in Figure 11. It is clear from the micrographs that a considerable difference exists in the degree of disturbance of the fibres at the fracture surfaces, with the carbon fibres experiencing significant fibre breakage and pull-out, and the glass/epoxy surface showing substantially lower surface roughness.
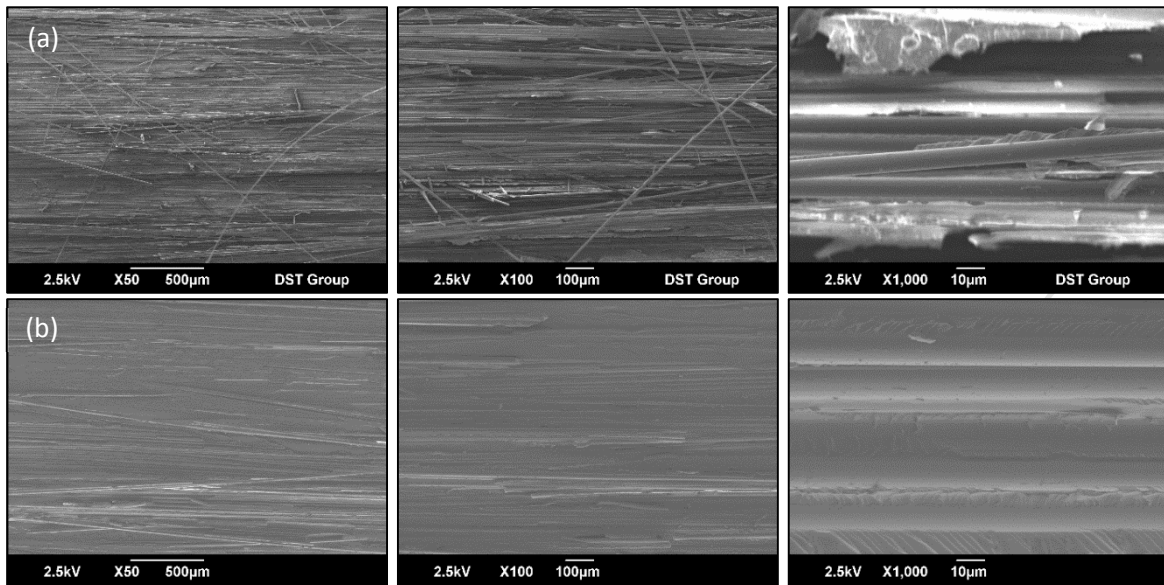
Figure 11. Electron micrographs acquired along the crack face in the (a) carbon/epoxy and

(b) glass/epoxy laminates. Magnification from left to right: x50, x100, x1000.

Figure 12 shows a nano-CT image of the fibre-resin interfaces through the plies in a glass/epoxy laminate. For the specimens investigated in this study, the plies were laid up unidirectionally at 0°, and hence there is some movement of the fibres between successive plies.
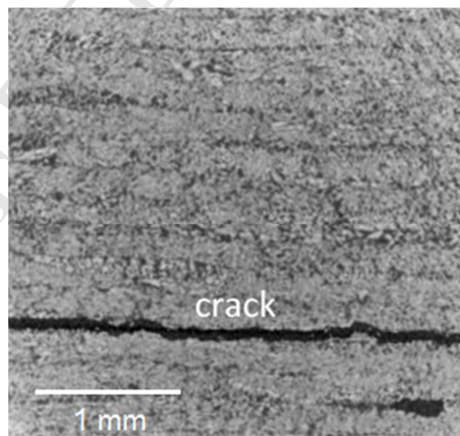

Figure 12. Nano-CT image of resin ply interface layers (horizontal) in a glass/epoxy laminate. Fibres run perpendicular to the page. Approximately 3.2 mm of the crack is shown. However, due to the unidirectional 0° layup, the distinction between successive plies is not always obvious.

4 Analysis and Discussion

4.1 Analysis of the full waveform

A close examination of the full waveform travelling through the composite specimens, in particular the uncracked laminate or the sub-laminate above the crack plane, reveals a noticeable change in the internal reflectivity of the glass plies prior to the crack echo. Figure 13 shows a series of reflection waveforms for a series of crack-opening displacements to a depth (time) pertaining to the back face of the laminate. For carbon/epoxy laminates, the waveforms before the crack reflection are closely superimposed, whereas the glass/epoxy waveform shows distinct differences from the point of entry into the composite through to the crack reflection. Here, the amplitudes of the internal reflections as well as the crack reflections decreased as the opening displacement increased.

In order for further analysis to be made on the waveform, the pre-crack signal was corrected by removing the low-frequency transducer excitation, via a simple quadratic correction to the signal amplitude. The combined effect of the material prior to the crack on the ultrasound beam was then measured by integrating the area under the curve for the full-wave-rectified signal, under the various loading conditions.
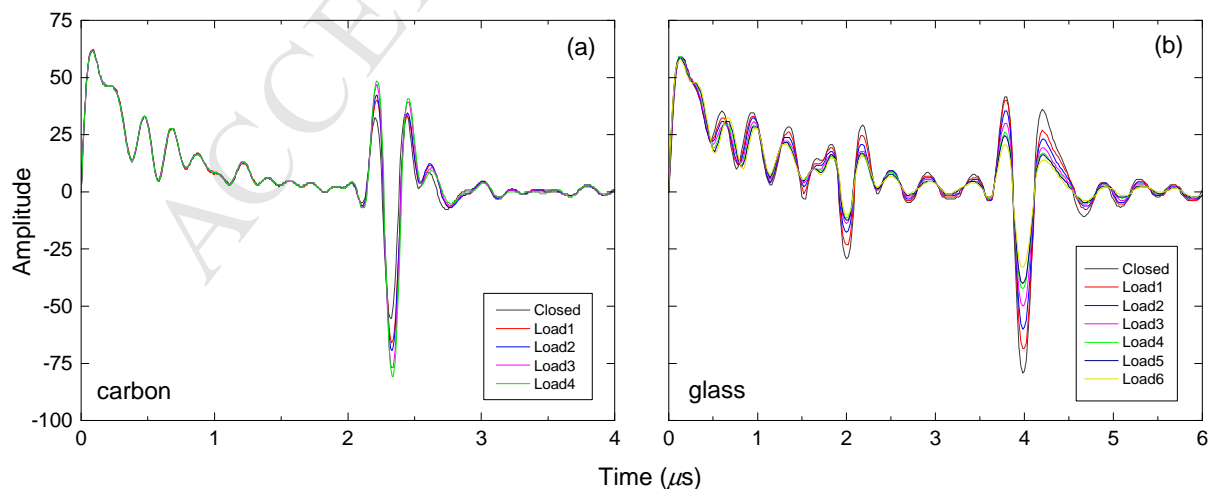
Figure 13. (a) Complete reflection waveform for carbon/epoxy specimen C4. (b) Complete reflection waveform for glass/epoxy specimen G6. The much larger variation in the early part of the waveform (prior to the crack reflection) on loading is obvious.

The cumulative areas under the reflection waveform curves for each of the loading states are shown in Figure 14. For the glass/epoxy composite, the behaviour of the ultrasonic response mimics the unexpected behaviour measured at the crack tip itself, in that the 'closed' state results in stronger reflections than any of the open states. The behaviour continues consistently as the waves travel through the composite. In the case of the carbon/epoxy specimens, the curves preceding the crack plane are independent of the loading condition, and differences are only observed beyond the crack tip depth. Hence, it can be deduced that this material effect is present throughout the loaded glass/epoxy laminate, rather than a directly-resultant effect caused by the measurement at the crack tip, and should be expected in glass-fibre laminates of similar construction. The material effect appears significant enough to negate the expected influence of the opening of the crack tip, as occurs for the carbon/epoxy composites. As the material effect occurs evenly in the through-thickness direction, its 'strength', relative to that of the expected increase from an open crack will be thickness-dependent. This issue will be particularly exacerbated in thick composite laminates, where a defect may be buried beneath several dozen, or even hundred, composite plies.
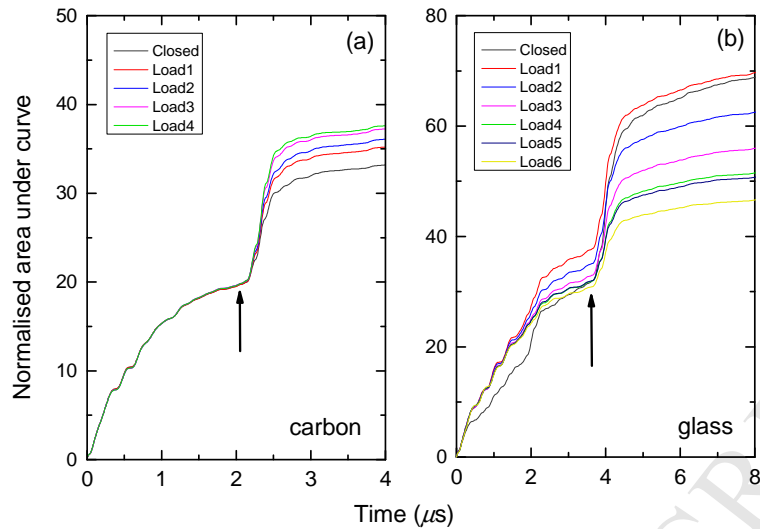
Figure 14. Cumulative area beneath the rectified (a) C4 carbon/epoxy and (b) G6 glass/epoxy ultrasonic signals for the thickness through which ultrasound is transmitted. The arrows indicate the point in time at which the crack signal appears. A clear variation between the glass/epoxy signals occurs prior to the crack plane, whereas the carbon/epoxy signals are identical in this regime.

4.2 Frequency spectra

The frequency spectra of the reflected ultrasonic waveforms were analysed in order to investigate the likelihood of the crack tip providing an energy storage mechanism in the early stages of crack opening. Figure 15 shows the frequency spectra obtained for a series of crack openings in typical carbon/epoxy and glass/epoxy laminates, and show a frequency response at the lower end of the input signal range (Figure 4b) in both cases. The peak response of the carbon-fibre laminate is at approximately 2.8 MHz, and at approximately 2.3 MHz in the glass-fibre laminate, both well below the centre frequency of the input signal. Of particular interest is the skew in the glass composite frequency response, possibly due to an unresolved higher harmonic peak that appears in the low load stages of the glass/epoxy specimens, until the signal reduction effect has been overcome by the significant opening of the crack tip, whereupon it weakens (see arrow indicating the location in Figure 15b). The difference in frequency spectra may provide some explanation for the apparent

20

difference in reflectance upon opening the crack in the glass laminate, and warrants further
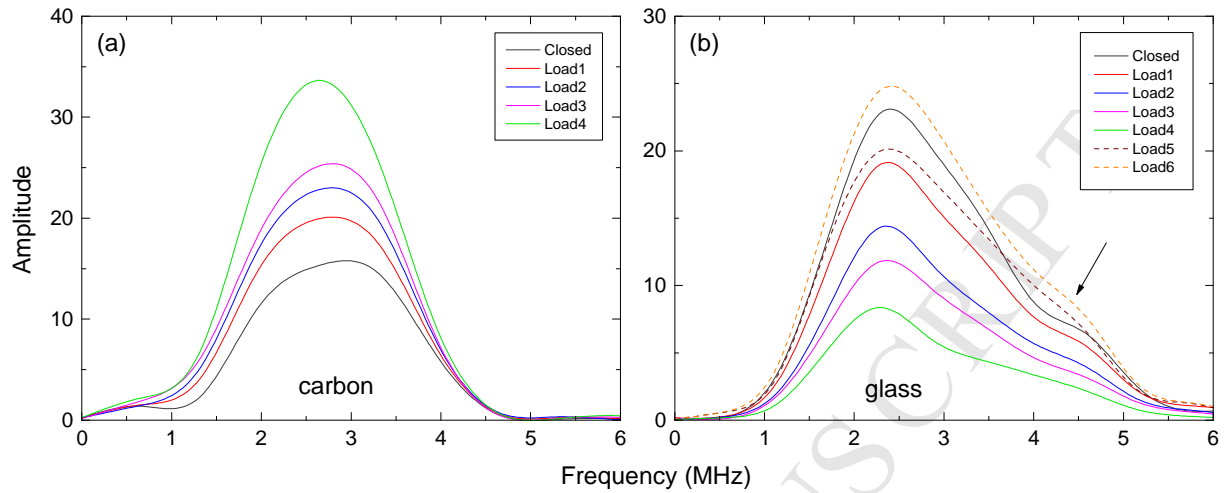
investigation.

Figure 15. Frequency spectra obtained via FFT for the crack reflection from two crack-opening series of (a) carbon/epoxy specimen C4 and (b) glass/epoxy specimen G6. The arrow indicates a possible higher-order effect in the glass laminate. The reverse amplitude increase in glass/epoxy is also clear in this colour series.

4.3 Instantaneous amplitude and phase of ultrasonic waveforms

The phase behaviour of the waveforms was studied by construction of the analytic signal via the

application of the Hilbert transform to the real (acquired) waveform signal, following the approach

of other authors [23,24]. The instantaneous amplitude is given by $Ae^{i\varphi} = Re(x) + i\,Im(x)$, where A

is the instantaneous amplitude, φ is the instantaneous phase, and $Re(x)$ is the real, measured

signal. The analytic signal of the echo response from the crack tip in a carbon/epoxy laminate is

shown in Figure 16, and provides insight into the true energy contained within the waveform.
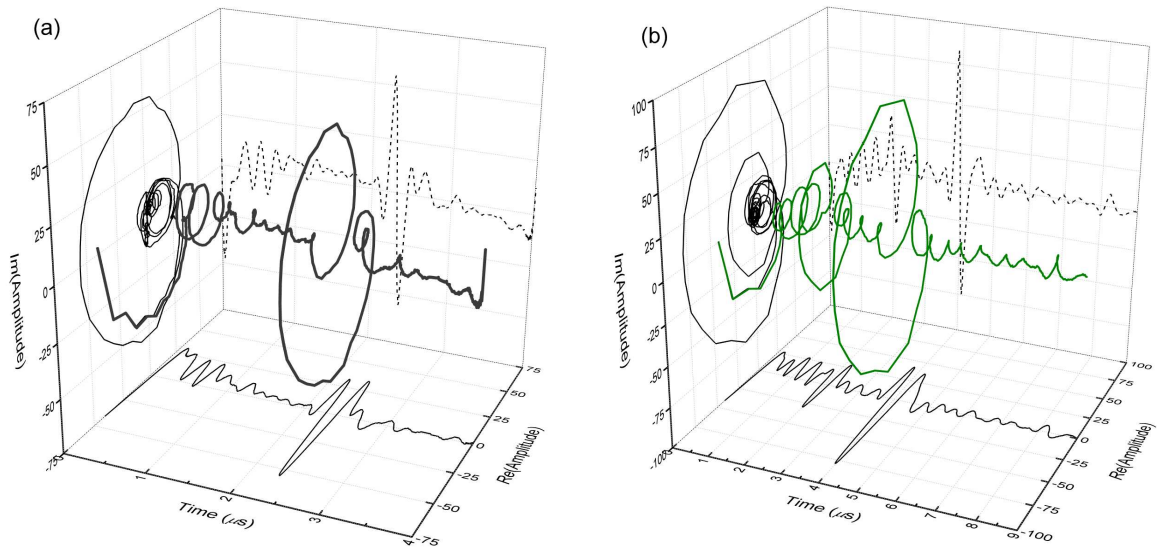
Figure 16. Real, imaginary and analytic signal for an ultrasonic pulse-echo response from

(a) carbon/epoxy specimen C4 and (b) glass/epoxy specimen G6. The large response from the crack

tip is at the centre of the waveforms.

Of particular interest is the real vs imaginary amplitude presentation, as shown in Figure 17. The

minor loops about the origin are not easily discernible when viewing the ultrasound through the

entire specimen in these realistic layups due to variations in the spacing and thickness of both the

ply and resin interface layers. The traces shown in the Figure are for the specimen with zero load.
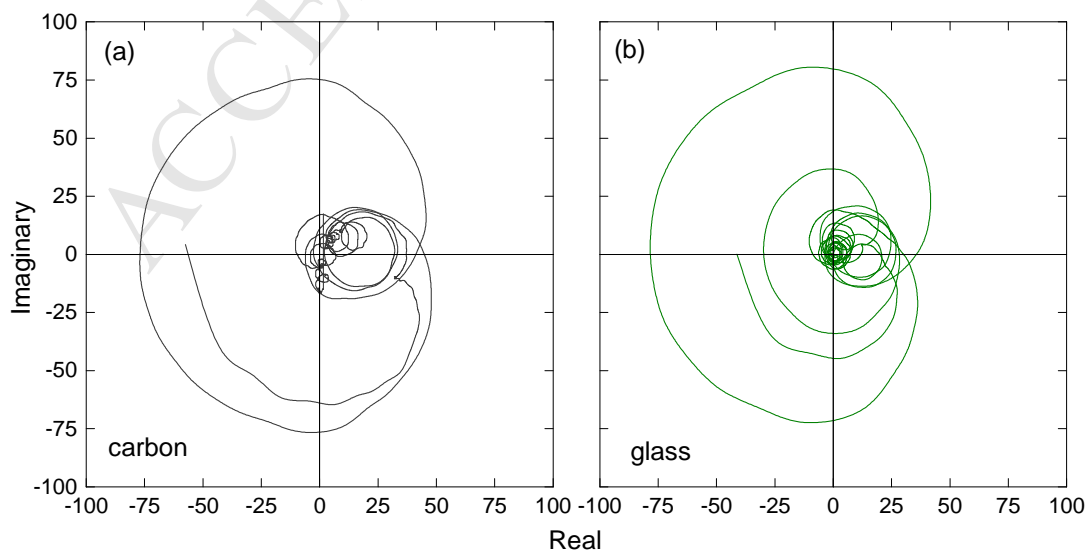
Figure 17. Normalised waveforms received from the (a) carbon/epoxy and (b) glass/epoxy composite laminates shown in Figure 16. The waveform timebase includes the period from introduction into the laminate through to the back wall, via a mid-plane crack, shown in a complex plane presentation.

Figure 18 shows a number of phase loops for crack-opening measurements made on carbon/epoxy and glass/epoxy specimens. The loops shown here include the crack reflection signal only, and the reverse amplitude behaviour between the carbon and glass composites is again obvious. The dashed line in Figure 18b indicates the load case where the signal amplitude has passed through the minimum value and increased to approximately the same level as for the closed crack (no load) state.
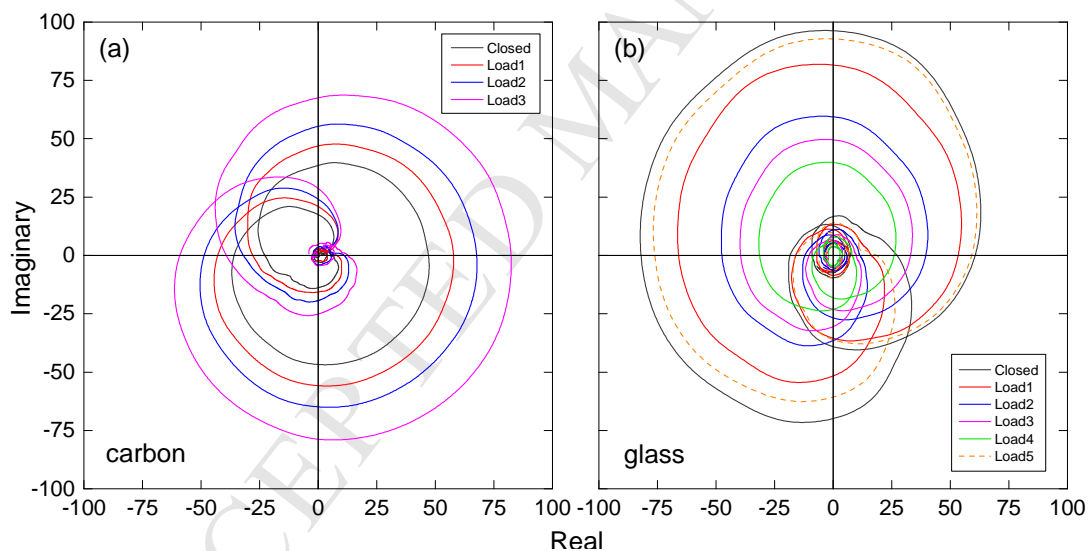

Figure 18. Normalised complex plane loops for the ultrasonic reflections for series of openings from the crack in (a) carbon/epoxy specimen C4 and (b) glass/epoxy specimen G3.

Immediately obvious is the significant phase rotation occurring between the carbon and glass composites, as well as the greater degree of variability in the phase rotation of the various load conditions in the glass composite. The "Load5" state in the glass/epoxy laminate (Figure 18b) shows

the case where the signal has returned to a similar amplitude to that of the specimen at rest, with a very similar form in the complex plane. The phase response in the glass/epoxy specimens is what would be expected from a normal resin layer under compression, as is the amplitude response, up to the higher loads. The change in response suggests a loading mechanism that closes the crack during the initial phases, although the exact nature of this behaviour has not yet been determined.

4.4   Destructive interference at the crack tip

A further mechanism that has relevance only at the crack tip may be the loss of sound energy due to a destructive interference via averaging over the full diameter of the piezoelectric transducer crystal, which was placed halfway over the visible part of the crack tip. The pulse-echo reflection from a resin-layer interface is out of phase with the reflection from a delamination or back-surface echo by $\pi/2$ [24], and the resin-layer reflection is significantly stronger in the glass/epoxy composite. Hence, there is a possibility that the response of the gradually-opening crack beneath the outer half of the beam interferes with the expected response from the open part of the crack. In the case of a phase difference of π between a slightly open crack and a very open crack, such interference would be a plausible explanation for the reduction in amplitude. This might be possible via the presence of an evanescent wave occurring in the air gap at the crack tip. At a sound speed in air 1/10 of that in the composite, a much smaller path length (~30 μm) is needed in order to contain one half wavelength. The increased smoothness of the glass/epoxy laminate fracture surface (Figure 11) may also contribute to this effect.

4.5   Thinning of the resin interface layer

A further mechanism that may contribute to the results obtained for the glass/epoxy laminates is the possible change in thickness of the resin interface layers under compressive stress, given the far

higher transverse stiffness of the glass fibres. The ultrasonic reflection coefficient shows an approximately linear relationship with resin layer thickness over the practical ultrasonic inspection frequency range, so a significant reduction in layer thickness would be required for this mechanism to play a major role in the changes to the signal (above a factor of 2) observed here. The degree to which this mechanism influences the signal may be verified by a stress analysis of the laminate in typical loading conditions.

5   Conclusions and Further Work

This study presents the first measurements quantifying the effect of crack closure on ultrasonic inspectability of delaminations in carbon/epoxy and glass/epoxy FRP laminates. For pulse-echo ultrasonic inspection of unidirectional laminates, carbon/epoxy composites exhibit an increase in reflection amplitude at the crack tip during crack opening. The glass/epoxy laminates studied exhibited an opposite response to the behaviour expected during the opening of a crack. Possible mechanisms have been identified, including the evanescent effect at the crack tip for small crack openings, leading to non-linear behaviour energy, and changes in reflectivity of the ultrasound due to the high stiffness gradient between the glass/epoxy composite and resin interface layers. Further study is required to identify which mechanism is the principal cause of the initial decrease in reflection amplitude during crack opening. The effects reported in this paper are of particular relevance to the inspection of thick-section composite laminates in which defective regions may lie beneath many dozens of plies, resulting in a multiplicative effect on detection and sizing errors for deeply buried defects.

This initial study highlights a number of areas for further study via modelling and experimental measurement, including: further examination of the behaviour in the closed portion of the crack tip via the application of highly focused ultrasound beams, and a possible improvement in the definition of the term 'closed', for the purposes of ultrasonic inspection; understanding the evanescent effect

25

that likely exists in the air gap of the opening crack to determine the relationship between transmitted/reflected energy and crack thickness; and a quantitative understanding of the relationship between the crosshead opening and the state of the crack tip during loading under a DCB configuration. Finally, a study of the effect of compressive stress on resin interface layers in glass/epoxy laminates is an important next step to quantitatively explain the unusual material effect within undamaged laminates, and to determine its influence in through-thickness ultrasonic measurements of glass FRP materials.

6   Acknowledgements

7   References

[1].   Ibrahim, M. E., *Compos. Part A: Appl. Sci. Manufact.* **64** 36-48 (2014).
[2].   Bar-Cohen, Y., *Mater. Eval.* **44** (4) 446-454 (1986).
[3].   Hagemaier, D. J. & Fassbender, R. H., *Mater. Eval.* **37** (7) 43-49 (1979).
[4].   Prakash, R., *Composites* **11** (4) 217-224 (1980).
[5].   Reynolds, W. N., *Mater. Design* **5** (6) 256-270 (1985).
[6].   Scott, I. G. & Scala, C. M., *NDT Int.* **15** (2) 75-86 (1982).
[7].   Smith, R. A., *Mater. Eval.* **65** (7) 697-710 (2007).
[8].   Stone, D. E. W., *Brit. J. Nondestr. Test.* **20** (2) 65-75 (1978).
[9].   Smith, R. A., Nelson, L. J., Mienczakowski, M. J., & Challis, R. E., *Proc. 17th International Committee on Composite Materials*, 2009).
[10].   Rokhlin, S. I. & Kim, J.-Y., *Int. J. Fatigue* **25** (1) 51-58 (2003).
[11].   Clark, R., Dover, W. D., & Bond, L. J., *NDT Int.* **20** (5) 269-275 (1987).
[12].   Bowles, S. J., Harding, C. A., & Hugo, G. R., in *Review of Progress in Quantitative Nondestructive Evaluation*, edited by Thompson, D. O. & Chimenti, D. E., Vol. 1096, pp. 1878-1885 (American Institute of Physics, 2009).
[13].   Makino, K., Biwa, S., Sakamoto, H., & Yohso, J., *Nondestruct. Test. Eval.* **27** (1) 29-46 (2012).
[14].   Donough, M. J., Gunnion, A. J., Orifici, A. C., & Wang, C. H., *Compos. Sci. Technol.* **120** 39-48 (2015).

[15]. Smith, R. A., *Insight* **36** (8) 595-605 (1994).

[16]. Chen, A. S., Almond, D. P., & Harris, B., *Compos. Sci. Technol.* **61** (16) 2437-2443 (2001).

[17]. Mode i interlaminar fracture toughness of unidirectional fiber-reinforced polymer matrix composites,(D5528-01), ASTM International,West Conshohocken, PA, USA (2007)

[18]. Smith, R. E., *J. Appl. Phys.* **43** (6) 2555-2561 (1972).

[19]. Lonne, S., Lhemery, A., & Thevenot, F., in *Review of Progress in Quantitative Nondestructive Evaluation*, ed. Thompson, D. O. and Chimenti, D. E., Vol. 23, pp. 898-905 (Springer, 2004).

[20]. Staab, G. H., *Laminar composites* (Butterworth-Heinemann, 2015).

[21]. Hashin, Z., *J. Appl. Mech.* **46** (3) 543-550 (1979).

[22]. Smith, R. A., *Use of 3D ultrasound data sets to map the localised properties of fibre-reinforced composites*, Ph.D. Thesis, School of Electrical and Electronic Engineering, The University of Nottingham (2010).

[23]. Picinbono, B., *IEEE Trans. Sig. Process.* **45** (3) 552-560 (1997).

[24]. Smith, R. A., Nelson, L. J., Mienczakowski, M. J., & Wilcox, P. D., in *Review of Progress in Quantitative Nondestructive Evaluation*, edited by Bond, L. J. & Chimenti, D. E., Vol. 1096, pp. 1878-1885 (American Institute of Physics, 2016).

Highlights

- Crack closure in fibre-reinforced laminates affects ultrasonic delamination sizing
- Pulse-echo reflections in carbon/epoxy increase with crack opening
- Pulse-echo reflections in glass/epoxy initially decrease with crack opening